MORPHOLOGICAL INSTABILITY AND KINETICS OF AN ELASTIC FILM ON A VISCOELASTIC LAYER

S.H. IM AND R. HUANG
Research Center for Mechanics of Solids, Structures & Materials
Department of Aerospace Engineering and Engineering Mechanics
The University of Texas, Austin, TX 78712, USA

Abstract

This paper develops a theoretical model for wrinkling of an elastic film on a viscoelastic layer. The film is elastic and subjected to a compressive residual strain. The viscoelastic layer is sandwiched between the film and a rigid substrate. The nonlinear von Karman plate theory is employed to model the film, and a thin-layer approximation is adopted for the viscoelastic layer. The stability of the system and the kinetics of structural evolution are studied first by a linear perturbation analysis and then by numerical simulations, both for plane strain deformation only. Three stages of evolution are identified: initial growth of the fastest growing mode, intermediate growth with mode transition, and finally an equilibrium wrinkled state. The results qualitatively agree with experimental observations of wrinkling in metal/polymer bilayer films.

1. Introduction

Complex wrinkle patterns have been observed in thin film systems with integrated compliant layers. The wrinkles are a nuisance in some applications (Iacopi *et al*., 2003; Yin *et al*., 2003), but may be used as stretchable interconnects for flexible electronics (Watanabe *et al*., 2002; Lacour *et al*., 2003), or biological assays (Cerda and Mahadevan, 2003). The wrinkle pattern can be controlled by engineering the surface structures or chemistry for micro to nanoscale fabrication (Bowden *et al*., 1998; Chua *et al*., 2000). It is also possible to extract mechanical properties (e.g., Young's modulus and residual stress) of thin film materials from wrinkle patterns (Martin *et al*., 2000; Stafford *et al*., 2004).

The underlying mechanism of wrinkling has been understood as a stress-driven instability, similar to Euler buckling of an elastic column under compression. For a solid film bonded to a substrate, however, the instability is constrained. If the substrate is elastic, there exists a critical compressive stress, beyond which the film wrinkles with a particular wavelength selected by minimizing the total elastic energy in the film and the substrate (Groenewold, 2001; Chen and Hutchinson, 2004; Huang *et al*., 2004). If the substrate is viscous, wrinkling becomes a kinetic process (Sridhar *et al*., 2001;

Huang and Suo, 2002A). Since the viscous substrate does not store elastic energy, a compressed blanket film is always unstable energetically. The viscous flow in the substrate controls the kinetics, selecting a fastest growing wavelength. More generally, if the substrate is viscoelastic, both energetics and kinetics play important roles. A spectrum of evolving wrinkle patterns has been observed experimentally in metal/polymer bilayers (Yoo and Lee, 2003), exhibiting a peculiar kinetic process. A linear perturbation analysis has shown that the viscoelastic property of the substrate significantly influences the wrinkling kinetics, even at the initial stage (Huang, 2005). This paper goes beyond the linear perturbation analysis and simulates the evolution of wrinkles in an elastic film on a thin viscoelastic layer.

2. Model Formulation

Figure 1 shows a model structure, an elastic film of thickness h_f lying on a viscoelastic layer of thickness H, which in turn lies on a rigid substrate. At the reference state (Fig. 1a), both the elastic film and the viscoelastic layer are flat, and the film is subjected to an in-plane biaxial compressive stress σ_0 (i.e, $\sigma_0 < 0$). Upon wrinkling (Fig. 1b), the film undergoes both in-plane and out-of-plane displacements, and the viscoelastic layer deforms concomitantly, with the interface assumed to remain bonded.

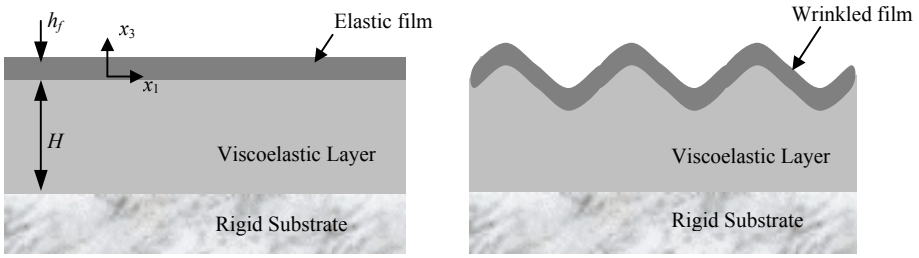

(a) Reference state (b) Wrinkled state

Figure 1. Schematic of a model structure

2.1 DEFORMATION OF AN ELASTIC FILM

Let w be the lateral deflection of the film, u_α the in-plane displacement ($\alpha = 1,2$), p the pressure at the interface, and τ_α the shear tractions. Employing the nonlinear von Karman plate theory, equilibrium requires that

$$p = D_f \frac{\partial^4 w}{\partial x_\alpha \partial x_\alpha \partial x_\beta \partial x_\beta} - N_{\alpha\beta} \frac{\partial^2 w}{\partial x_\alpha \partial x_\beta} - \tau_\alpha \frac{\partial w}{\partial x_\alpha}, \tag{1}$$

$$\tau_\alpha = \frac{\partial N_{\alpha\beta}}{\partial x_\beta}, \tag{2}$$

where

$$D_f = \frac{E_f h_f^3}{12(1-\nu_f^2)}, \tag{3}$$

$$N_{\alpha\beta} = \sigma_0 h_f \delta_{\alpha\beta} + \frac{E_f h_f}{1-\nu_f^2}\left[(1-\nu_f)\varepsilon_{\alpha\beta} + \nu_f \varepsilon_{\gamma\gamma}\delta_{\alpha\beta}\right], \tag{4}$$

$$\varepsilon_{\alpha\beta} = \frac{1}{2}\left(\frac{\partial u_\alpha}{\partial x_\beta} + \frac{\partial u_\beta}{\partial x_\alpha}\right) + \frac{1}{2}\frac{\partial w}{\partial x_\alpha}\frac{\partial w}{\partial x_\beta}. \tag{5}$$

Here E_f is the Young's modulus of the film, ν_f the Poisson's ratio, $N_{\alpha\beta}$ the in-plane membrane force, $\varepsilon_{\alpha\beta}$ the in-plane strain, $\delta_{\alpha\beta}$ the Kronecker delta. The Greek subscripts α and β take on the values of in-plane coordinates 1 and 2, and a repeated Greek subscript implies summation over 1 and 2. Note that, both the in-plane displacements and the deflection contribute to the relaxation of the compressive stress. The nonlinear term in Eq. (5) accounts for moderately large deflection of the film.

2.2 DEFORMATION OF A VISCOELASTIC THIN-LAYER

The underlayer material is assumed to be isotropic, linear viscoelastic, with a relaxation modulus $\mu(t)$ and Poisson's ratio $\nu(t)$. The layer is stress free initially ($t = 0$) and subjected to a normal and a shear traction at the top surface for $t > 0$, namely

$$\sigma_{31} = S_1(x_1, t) \text{ and } \sigma_{33} = S_3(x_1, t) \text{ at } x_3 = 0. \tag{6}$$

At the lower surface, the displacement is fixed:

$$u_1 = u_3 = 0 \text{ at } x_3 = -H. \tag{7}$$

Consider a periodic traction in the form of

$$S_1(x_1, t) = A(t)\sin kx_1, \tag{8}$$

$$S_3(x_1, t) = B(t)\cos kx_1, \tag{9}$$

where k is the wave number, $A(t)$ and $B(t)$ are the amplitudes. The plane-strain deformation of a viscoelastic layer subjected to such a periodic surface traction has been solved by Huang (2005) using Laplace transform and the correspondence principle of viscoelasticity. The Laplace transform of the displacements at the top surface are

$$\overline{u}_1(x_1, s) = \frac{1}{2ks\overline{\mu}(s)}\left[\gamma_{11}(s\overline{\nu}, kH)\overline{A}(s) + \gamma_{12}(s\overline{\nu}, kH)\overline{B}(s)\right]\sin(kx_1), \tag{10}$$

$$\overline{u}_3(x_1, s) = \frac{1}{2ks\overline{\mu}(s)}\left[\gamma_{21}(s\overline{\nu}, kH)\overline{A}(s) + \gamma_{22}(s\overline{\nu}, kH)\overline{B}(s)\right]\cos(kx_1), \tag{11}$$

where

$$\gamma_{11} = \frac{1+\kappa}{4}\frac{\kappa\sinh(2kH) + 2kH}{\kappa\cosh^2(kH) + (kH)^2 + \left(\frac{1-\kappa}{2}\right)^2}, \tag{12}$$

$$\gamma_{22} = \frac{1+\kappa}{4}\frac{\kappa\sinh(2kH) - 2kH}{\kappa\cosh^2(kH) + (kH)^2 + \left(\frac{1-\kappa}{2}\right)^2}, \tag{13}$$

$$\gamma_{12} = \gamma_{21} = -\frac{\frac{\kappa(1-\kappa)}{2}\sinh^2(2kH) + (kH)^2}{\kappa\cosh^2(kH) + (kH)^2 + \left(\frac{1-\kappa}{2}\right)^2}, \tag{14}$$

and $\kappa = 3 - 4s\overline{\nu}(s)$. A bar over a variable designates its Laplace transform, and s is the transform variable.

In general, the surface of the viscoelastic layer undergoes both out-of-plane and in-plane displacements and they are coupled. The coupling is broken in two special cases, one for an infinitely thick ($kH \to \infty$) and incompressible ($\nu = 0.5$) layer and the other for a very thin layer ($kH \to 0$). The former has been considered previously (Huang, 2005). This paper considers the thin layer limit, for which Eqs. (10) and (11) reduce to

$$\overline{u}_1(x_1, s) = \frac{1}{2ks\overline{\mu}(s)}\left[2kH\overline{A}(s) - \frac{1-4\nu}{2(1-\nu)}(kH)^2\overline{B}(s)\right]\sin(kx_1), \tag{15}$$

$$\overline{u}_3(x_1, s) = \frac{1}{2ks\overline{\mu}(s)}\left[\frac{1-2\nu}{1-\nu}(kH)\overline{B}(s) - \frac{1-4\nu}{2(1-\nu)}(kH)^2\overline{A}(s)\right]\cos(kx_1), \tag{16}$$

where only the leading terms in kH are retained and the Poisson's ratio has been assumed to be a constant independent of time. In addition, $\nu \neq 0.5$ is assumed. As will be shown in a subsequent study, the kinetics is quite different if the underlayer is incompressible (i.e., $\nu = 0.5$).

The surface displacement as a function of time is obtained by the inverse Laplace transform of Eqs. (15) and (16). To be specific, consider the Kelvin model of viscoelasticity with a spring and a dashpot in parallel, for which the relaxation modulus is,

$$\mu(t) = \mu_\infty + \eta\delta(t), \tag{17}$$

where μ_∞ is the elastic shear modulus at the rubbery limit and η is the viscosity. The Laplace transform of the relaxation modulus is

$$\overline{\mu}(s) = \frac{\mu_\infty}{s} + \eta. \tag{18}$$

After substituting (18) into Eqs. (15) and (16), the inverse Laplace transform leads to

$$\frac{\partial u_1}{\partial t} = \frac{H}{\eta}S_1 - \frac{1-4\nu}{4(1-\nu)}\frac{H^2}{\eta}\frac{\partial S_3}{\partial x_1} - \frac{\mu_\infty}{\eta}u_1, \tag{19}$$

$$\frac{\partial u_3}{\partial t} = \frac{1-2\nu}{2(1-\nu)}\frac{H}{\eta}S_3 + \frac{1-4\nu}{4(1-\nu)}\frac{H^2}{\eta}\frac{\partial S_1}{\partial x_1} - \frac{\mu_\infty}{\eta}u_3. \tag{20}$$

Note that, in case of incompressible materials ($\nu = 0.5$), the first term at the right hand side of Eq. (20) vanishes. Using the next leading term of kH in Eq. (16), Eq. (20) becomes

$$\frac{\partial u_3}{\partial t} = -\frac{H^3}{3\eta}\frac{\partial^2 S_3}{\partial x_1^2} - \frac{H^2}{2\eta}\frac{\partial S_1}{\partial x_1} - \frac{\mu_\infty}{\eta}u_3. \tag{21}$$

Equations (19) and (21) are similar to those for a thin liquid layer by Reynold's lubrication theory (Huang and Suo, 2002A), but with an additional term accounting for the elastic limit.

Assuming $\nu \neq 0.5$ and neglecting the H^2 terms in Eqs. (19) and (20) as a thin-layer approximation, we obtain that

$$\frac{\partial u_1}{\partial t} = \frac{H}{\eta} S_1 - \frac{\mu_\infty}{\eta} u_1 , \tag{22}$$

$$\frac{\partial u_3}{\partial t} = \frac{1-2\nu}{2(1-\nu)} \frac{H}{\eta} S_3 - \frac{\mu_\infty}{\eta} u_3 . \tag{23}$$

Equation (22) is a combination of the shear lag model for elastic and viscous layers (Xia and Hutchinson, 2000; Huang *et al*., 2002), and Eq. (23) is similar to the Winkler model for elastic foundation (Allen, 1969) but includes a viscous term. The two equations are uncoupled under the thin-layer approximation.

In the development of Eqs. (22) and (23), plane strain deformation and periodic tractions have been assumed. The restriction of periodic tractions have been relaxed by linear superposition of all Fourier components in the form of (8) and (9). The restriction of plane strain deformation can also be relaxed by including the other in-plane component in the same form as Eq. (22), which leads to

$$\frac{\partial u_\alpha}{\partial t} = \frac{H}{\eta} S_\alpha - \frac{\mu_\infty}{\eta} u_\alpha , \tag{24}$$

for $\alpha = 1,2$.

2.3 COUPLED EVOLUTION EQUATIONS

The interface between the elastic film and the viscoelastic layer is assumed to remain bonded during deformation. Consequently, the displacements and the tractions are continuous across the interface. Therefore, the equilibrium equations (1) and (2) are coupled with Eqs. (23) and (24), leading to

$$\frac{\partial w}{\partial t} = \frac{1-2\nu}{2(1-\nu)} \frac{H}{\eta} \left(- D_f \frac{\partial^4 w}{\partial x_\alpha \partial x_\alpha \partial x_\beta \partial x_\beta} + N_{\alpha\beta} \frac{\partial^2 w}{\partial x_\alpha \partial x_\beta} + \frac{\partial N_{\alpha\beta}}{\partial x_\beta} \frac{\partial w}{\partial x_\alpha} \right) - \frac{\mu_\infty}{\eta} w , \tag{25}$$

$$\frac{\partial u_\alpha}{\partial t} = \frac{H}{\eta} \frac{\partial N_{\alpha\beta}}{\partial x_\beta} - \frac{\mu_\infty}{\eta} u_\alpha . \tag{26}$$

Equations (25) and (26) are coupled, nonlinear evolution equations, which can be solved numerically to simulate the evolution of two-dimensional wrinkles. In the remainder of this paper, however, we consider one-dimensional plane-strain wrinkles only, for which some analytical solutions can be obtained to provide useful insights. The reduced equations for the plane-strain wrinkles are summarized as below:

$$\frac{\partial w}{\partial t} = \frac{1-2\nu}{2(1-\nu)} \frac{H}{\eta} \left(- D_f \frac{\partial^4 w}{\partial x^4} + N \frac{\partial^2 w}{\partial x^2} + \frac{\partial N}{\partial x} \frac{\partial w}{\partial x} \right) - \frac{\mu_\infty}{\eta} w , \tag{27}$$

$$\frac{\partial u}{\partial t} = \frac{H}{\eta} \frac{\partial N}{\partial x} - \frac{\mu_\infty}{\eta} u , \tag{28}$$

$$N = \sigma_0 h_f + \frac{E_f h_f}{1-\nu_f^2} \left[\frac{\partial u}{\partial x} + \frac{1}{2} \left(\frac{\partial w}{\partial x} \right)^2 \right] . \tag{29}$$

3. Linear Perturbation Analysis

Assume a small deflection from the reference state in the form of

$$w(x,t) = A(t)\cos kx\,. \tag{30}$$

The in-plane displacement is uncoupled from the lateral deflection in the linear perturbation analysis and therefore ignored. Inserting (30) into Eq. (27) and retaining only the leading order terms in A, we obtain that

$$\frac{dA}{dt} = \frac{\alpha E_f - \mu_\infty}{\eta} A(t)\,, \tag{31}$$

where,

$$\alpha = \frac{(1-2\nu)k^2 H h_f}{24(1-\nu)(1-\nu_f^2)}\left[-k^2 h_f^2 - \frac{12(1-\nu_f^2)\sigma_0}{E_f}\right]. \tag{32}$$

Solving Eq. (31) leads to

$$A(t) = A_0 \exp(s\frac{t}{\tau})\,, \tag{33}$$

where $\tau = \eta/E_f$ is the time scale and $s = \alpha - \mu_\infty/E_f$ is the dimensionless growth rate. Figure 2 plots the growth rate as a function of the wavelength ($L = 2\pi/k$) of the perturbation for various ratios between the rubbery modulus of the viscoelastic layer and the elastic modulus of the film. For a given residual stress in the film, there exists a critical ratio between the moduli, above which the growth rate is negative for all wavelengths and the film is stable against any perturbation. By setting the maximum growth rate to be zero, we find the critical ratio

$$\left(\frac{\mu_\infty}{E_f}\right)_c = \frac{3(1-\nu_f{}^2)(1-2\nu)}{2(1-\nu)}\frac{H}{h_f}\left(\frac{\sigma_0}{E_f}\right)^2. \tag{34}$$

In figure 2, the critical modulus ratio is 0.00025. For smaller modulus ratios, however, the growth rate is positive for intermediate wavelengths within a window bounded by two critical values; the film becomes unstable and a small perturbation grows to form wrinkles. The wavelength of the fastest growing mode is

$$L_m = \pi h_f \sqrt{-\frac{2E_f}{3(1-\nu_f^2)\sigma_0}}\,, \tag{35}$$

which is indicated by the dashed line ($L_m = 26.9h_f$) in Figure 2.

The effects of the viscoelastic layer on the stability of the elastic film can be drawn from the above analysis. The critical condition for the flat film to remain stable is controlled by the rubbery modulus of the underlayer, as given by Eq. (34). In cases that the film is unstable, the growth time scale is proportional to the viscosity and the growth rate increases as the rubbery modulus decreases. However, the wavelength of the fastest growing mode is independent of the underlayer properties, as given in Eq. (35). A similar analysis was conducted for a film on an incompressible viscous layer (Huang and Suo, 2002B), which led to a slightly smaller fastest growing wavelength; the difference is due to the incompressibility of the viscous liquid.

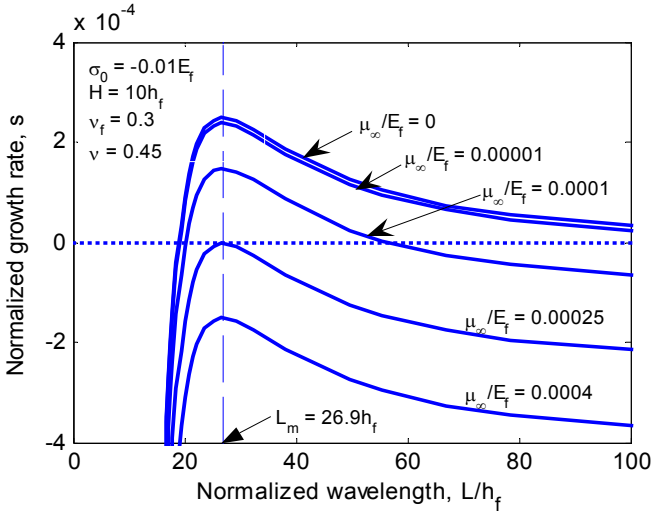

Figure 2: The dimensionless growth rate by the linear perturbation analysis.

4. Equilibrium Wrinkles

Setting $\partial/\partial t = 0$ in Eqs. (27) and (28) leads to two coupled nonlinear ordinary differential equations, from which one can solve for the equilibrium state. An approximate solution has been obtained by neglecting the in-plane displacement and the shear traction (Huang, 2005), from which the equilibrium amplitude of a sinusoidal wrinkle is

$$A_{eq} = \frac{2\sqrt{1-\nu_f^{\,2}}}{k}\left[-\frac{\sigma_0}{E_f} - \frac{(kh_f)^2}{12(1-\nu_f^{\,2})} - \frac{2(1-\nu)}{1-2\nu}\frac{\mu_\infty}{E_f}\frac{1}{k^2 H h_f}\right]^{1/2}. \qquad (36)$$

It can be confirmed that only when the film is unstable does there exist a nontrivial solution corresponding to the equilibrium wrinkled state.

Furthermore, at the equilibrium state, the wrinkle selects a wavelength that minimizes the elastic energy, namely,

$$L_{eq} = \pi h_f \left[\frac{2(1-2\nu)}{3(1-\nu)(1-\nu_f^2)}\frac{E_f}{\mu_\infty}\frac{H}{h_f}\right]^{1/4}. \qquad (37)$$

The equilibrium state is identical to that for a film on a thin elastic layer with the shear modulus μ_∞ (Huang *et al*., 2004). For a viscoelastic layer with zero rubbery modulus, however, the equilibrium wavelength approaches infinity. Consequently, the wrinkle wavelength coarsens indefinitely.

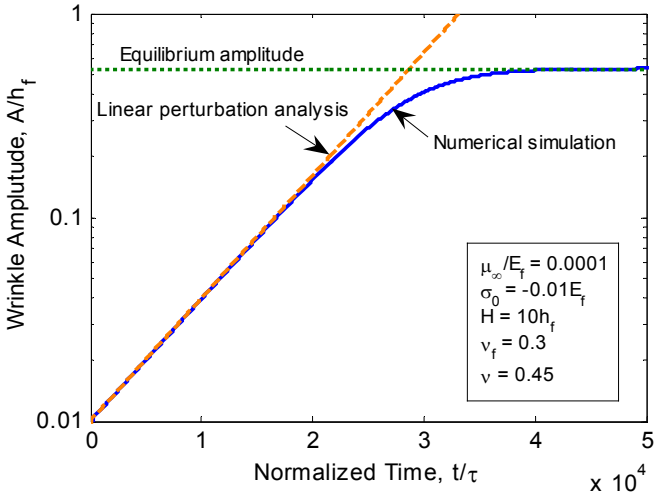

Figure 3: Growth of the amplitude of a sinusoidal wrinkle with wavelength $L = 30h_f$.

5. Numerical Simulations

In this section, we simulate the wrinkling process by integrating Equations (27) and (28) numerically with a finite difference method. First, a sinusoidal perturbation is assumed for the initial deflection. The wavelength was selected to be close to the fastest growing wavelength and it remains constant for the entire period of simulation. The amplitude grows over time, first exponentially and then approaching a constant corresponding to the equilibrium amplitude, as shown in Figure 3. The time is normalized by the time scale $\tau = \eta / E_f$. The exponential growth predicted by the linear perturbation analysis is plotted as the dashed line in Figure 3, and the equilibrium amplitude corresponding to the selected wavelength ($L = 30h_f$, $A_{eq} = 0.537h_f$) is indicated by the horizontal dotted line. The numerical simulation confirms the validity of the linear perturbation analysis at the initial stage and the equilibrium wrinkle amplitude of a particular wavelength.

Next, a random perturbation is generated for the initial deflection. Figure 4 shows the evolving deflection curves and their Fourier transforms. Figure 5 plots the evolution of the dominant wavelength (maximum intensity in the Fourier transform), and Figure 6 shows the growth of the RMS (i.e., the root mean square value). While many wavelengths co-exist in the initial perturbation, only those of intermediate wavelengths grow and the fastest growing wavelength ($L_m = 26.9h_f$) dominates at the initial stage. Three stages of the wrinkle evolution are identified: initial growth of the fastest growing mode, intermediate growth with mode transition, and finally an equilibrium wrinkled state. For $\mu_\infty / E_f = 0.00001$, the equilibrium wrinkle has a wavelength $L_{eq} = 60.0h_f$ and an amplitude $A_{eq} = 1.63h_f$ (RMS = $1.15h_f$). Such behavior qualitatively agrees with the experimental observations in a metal/polymer bilayer film (Yoo and Lee, 2003).

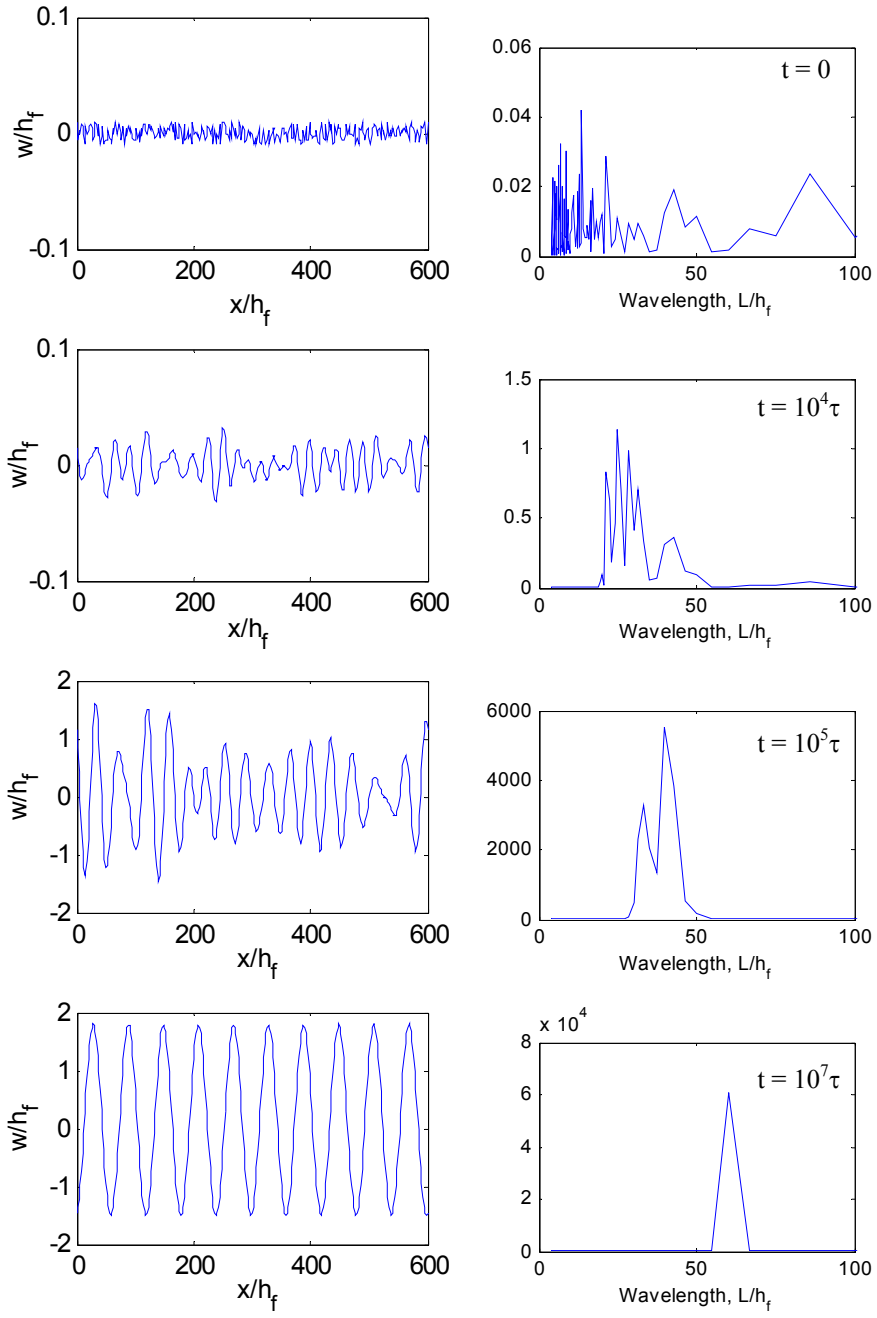

Figure 4: Simulated evolution of wrinkles (left) and their Fourier transform (right).

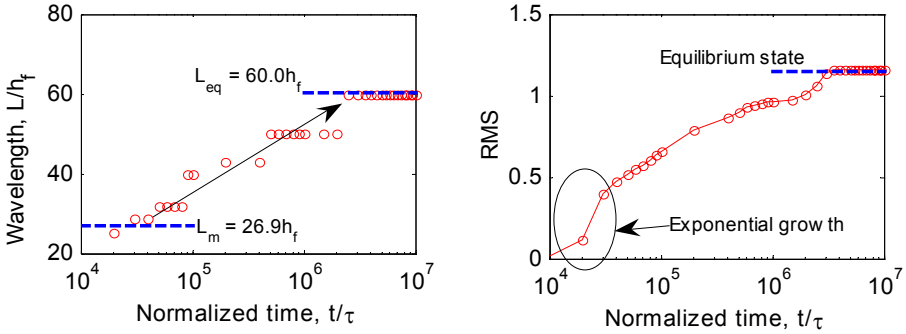

Figure 5: Simulated evolution of the dominated wavelength (left) and the RMS of a wrinkled film on a viscoelastic layer.

References

Allen, H.G., 1969. Analysis and Design of Structural Sandwich Panels, Pergamon, New York.

Bowden, N., Brittain, S., Evans, A.G., Hutchinson, J.W., Whitesides, G.M., 1998. Spontaneous formation of ordered structures in thin films of metals supported on an elastomeric polymer. Nature 393, 146-149.

Cerda, E. and Mahadevan, L., 2003. Geometry and physics of wrinkling. Phys. Rev. Lett. 90, 074302.

Chen, X. and Hutchinson, J.W., 2004. Herringbone buckling patterns of compressed thin films on compliant substrates. J..Appl. Mech., in press.

Chua, D.B.H., Ng, H.T., Li, S.F.Y., 2000. Spontaneous formation of complex and ordered structures on oxygen-plasma-treated elastometric polydimenthylsiloxane. Applied Physics Letters 76, 721-723.

Groenewold, J., 2001. Wrinkling of plates coupled with soft elastic media. Physica A 298, 32-45.

Huang, R., 2005. Kinetic Wrinkling of an Elastic Film on a viscoelastic Substrate. J. Mech. Phys. Solids 53, 63-89.

Huang, R., Prevost, J.H., Suo, Z., 2002. Loss of constraint on fracture in thin film structures due to creep. Acta Mater. 50, 4137-4148.

Huang, R. and Suo, Z., 2002A. Wrinkling of an elastic film on a viscous layer. J. Appl. Phys. 91, 1135-1142.

Huang, R. and Suo, Z., 2002B. Instability of a compressed elastic film on a viscous layer. Int. J. Solids Struct. 39, 1791-1802.

Huang, Z.Y., Hong, W., Suo, Z., 2004. Nonlinear analysis of wrinkles in films on soft elastic substrates. Submitted.

Iacopi, F., Brongersma, S.H., Maex, K., 2003. Compressive stress relaxation through buckling of a low-k polymer-thin cap layer system. Appl. Phys. Lett. 82, 1380-1382.

Lacour, S.P., Wagner, S., Huang, Z.Y., Suo, Z., 2003. Stretchable gold conductors on elastomeric substrates. Appl. Phys. Lett. 82, 2404-2406.

Martin, S.J., Godschalx, J.P., Mills, M.E., Shaffer II, E.O., Townsend, P.H., 2000. Development of a low-dielectric-constant polymer for the fabrication of integrated circuit interconnect. Advanced Materials 12, 1769-1778.

Sridhar, N., Srolovitz, D.J., Suo, Z., 2001. Kinetics of buckling of a compressed film on a viscous substrate. Appl. Phys. Lett. 78, 2482–2484.

Stafford, C.M., Harrison, C., Beers, K.L., Karim, A., Amis, E.J., Vanlandingham, M.R., Kim, H.-C., Volksen, W., Miller, R.D., Simonyi, E.E., 2004. A buckling-based metrology for measuring the elastic moduli of polymeric thin films. Nature Materials 3, 545-550.

Watanabe, M., Shirai, H., Hirai, T., 2002. Wrinkled polypyrrole electrode for electroactive polymer actuators. J. Appl. Phys. 92, 4631-4637.

Xia, Z.C. and Hutchinson, J.W., 2000. Crack patterns in thin films. J. Mech. Phys. Solids 48, 1107-1131.

Yin, H., Huang, R., Hobart, K.D., Liang, J., Suo, Z., Shieh, S.R., Duffy, T.S., Kub, F.J., Sturm, J.C., 2003. Buckling suppression of SiGe islands on compliant substrates. J. Appl. Phys. 94, 6875-6888.

Yoo, P.J. and Lee, H.H., 2003. Evolution of a stress-driven pattern in thin bilayer films: spinodal wrinkling. Phys. Rev. Lett. 91, 154502.